Atomistic approach for Boron Transient enhanced diffusion and clustering

Aurelio Mauri*, Luca Laurin†, Francesco Montalenti† and Augusto Benvenuti*
* Central R&D STMicroelectronics M6, Agrate Brianza Italy email: aurelio.mauri@numonyx.com
† Materials Science Department University of Milano Bicocca, Milano Italy email: francesco.montalenti@unimib.it

Abstract—**A Kinetic Monte Carlo (KMC) approach has been applied to study the thermal evolution of Boron implant damage and diffusion in bulk silicon in a wide range of temperatures between 700°C and 1100°C, considering furnace, rapid thermal and spike annealing. Boron Transient Enhanced Diffusion (TED) and boron interstitial clustering (up to B_3I_3) have been considered with a consistent set of parameters for all the standard anneal cases, achieving a satisfactory agreement with experimental profiles and providing a good understanding of the main underlying microscopic mechanisms.**

I. Introduction

In the past 20 years great attention has been devoted to model Boron TED and activation mainly driven by the need of an accurate description of the process to obtain low resistance shallow juntions for advanced CMOS architecture. Using continuum simulators several authors have proposed different Boron Interstitial Clusters (BICs) models trying to reduce the number of equations needed to reproduce the experimental chemical (SIMS) and activation (spreading reasistance) profiles [1] [2] . Our approach is based on a KineticMonteCarlo (KMC) code, which, with respect to continuum simulation, allowed us to consider a larger number of microscopic interactions between boron, silicon interstitials and boron interstitial clusters. Such a complex interplay controls the interstitial supersaturation and Boron TED.

II. Modeling Approach

We have used a commercial KineticMontercarlo code [3] that gives an open platform in term of particle species, interactions and agglomeration based on the Harmonic Transistion State Theory approximation of the event rates. The charge state of point defects and pairs has been accounted for considering the contribution of neutral, negatively and positively charged boron interstitistials (Bi) to Boron diffusion under intrinsic and extrinsic conditions. Since in all cases a thin SiO_2 capping layer was present we have used the well-known three-phase segregation model already implemented in [3] to reproduce Boron segregation: a careful calibration of boron interaction with trapping sites at the interface and of boron migration in oxide was needed to better reproduce the experimental data. At this stage of the implememtation we have considered only B_mI_n clusters with m,n $\leq$ 3 with different reactions, as reported in table I, with the purpose of a simplified translation in a continuum modeling framework. All the clusters (BICs and I clusters) are assumed to be immobile. In order to have a good statistical ensemble for each simulated curve we have performed a large number of simulations with different seeds to initialize the MC algorithm and extract the resulting average profile. After calibration a unique set of interactions and parameters has been used for all the considered furnace and rapid thermal treatments, while in order to accurately describe spike anneal profiles a slight correction of BICs emission energies has been employed keeping the same overall modelling framework (e.g. BICs species and interactions, point defect parameters, migration barriers).

III. Results

In order to calibrate the model we have considered medium and high dose (from 1e14 at/cm^2 to 2e15 at/cm^2) Boron implant at ultra-low and low energy (between 0.5-20 KeV) followed by inert annealings (furnace, RTP and spike anneal) in a temperature range between 700°C and 1100°C

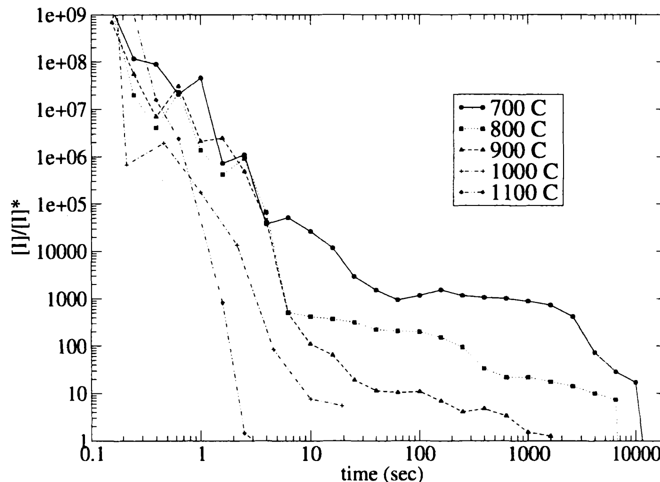

Figure 1: Time evolution of interstitial super saturation. For spike anneal treatments excess Si vanishes already during ramp-up.

Due to its relevance for Boron TED, silicon interstitial super-saturation is shown in fig. 1 as a function of time and temperature for all the experiments. With respect to the default parameter set reported in [3] we adjusted the interstitial equilibrium concentration and the minimum size of {311} defects in order to better match the TED behaviour on a larger temperature range and to reproduce the {311} dissolution kinetic in agreement with [4]. Moreover {311} and dislocation loops formation/dissolution has been correctly described as shown in ref. [5]. In figs. 2 and 3 atomistic simulations have

been compared with experimental data at low temperature: B 1e14 at/cm^2 at 10keV and B 5e14 at/cm^2 at 20keV with a four hours anneal at 700°C and 750°C respectively (data from ref. [6]). The immobile peak is quite well reproduced due to the B_3I and B_3I_2 clusters.

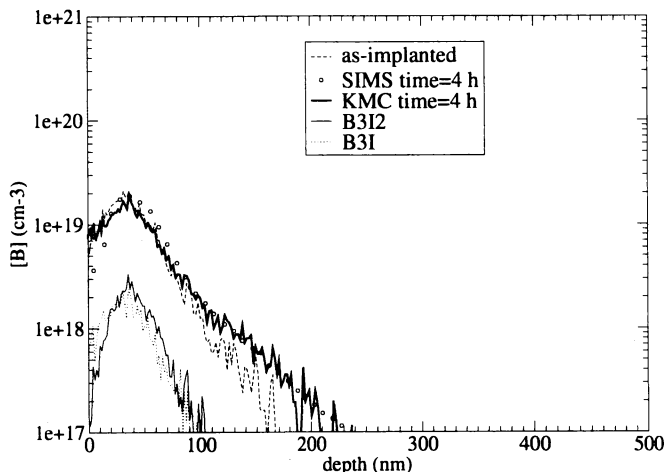

Figure 2: Boron diffusion at 700°C (B 1e14 at/cm^2 at 10keV), ref. [6].

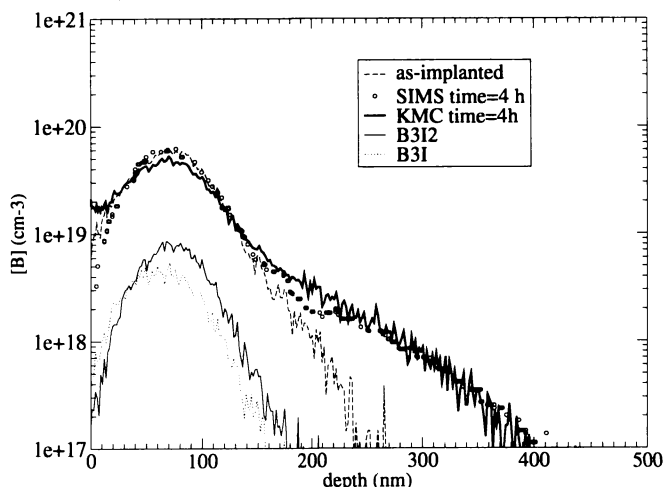

Figure 3: Boron diffusion at 750°C (B 5e14 at/cm^2 at 20keV), ref. [6].

In fig. 4 experimental data (ref. [7]) and simulation results are shown for the case of B 5e14 at/cm^2 at 20keV for annealing time between 5 and 30 min at 800°C : the immobile peak has been reproduced quite well. It seems that TED is slightly underestimated, but cases with high implanted dose (2e15 at/cm^2) don't show this problem.

In fig. 5 SIMS profiles (ref. [7]) and atomistic simulations are shown for a five minutes anneal at 850°C for an implant of B 2e15 at/cm^2 at 20keV. Again B_3I and B_3I_2 are responsible for the immobile peak (the activation of Boron has been estimated to be around 83%).

To understand the effect of our calibration on the micro-scopic interaction, the BICs evolution is shown in fig. 6 at 800°C : as revealed by the simulations B_3I and B_3I_2 are the

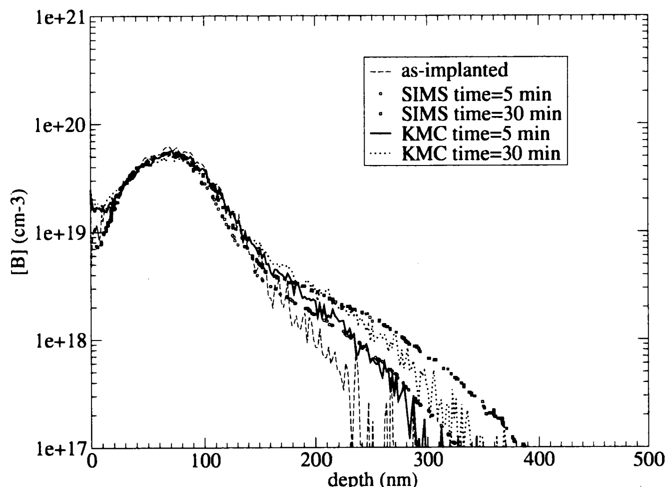

Figure 4: Boron diffusion at 800°C (B 5e14 at/cm^2 at 20keV), ref. [7].

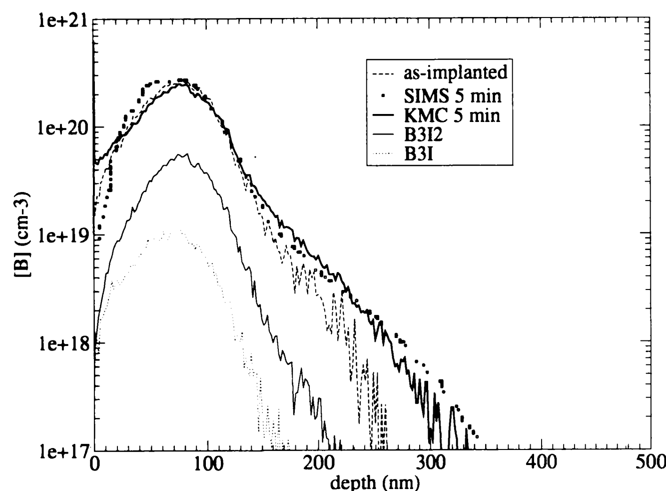

Figure 5: Boron diffusion at 850°C (B 2e15 at/cm^2 at 20keV), ref. [7].

only surviving BIC species for long time, low temperature annealing conditions. In fact at the initial stage just after implantation BI_2 clusters are formed. These clusters are not stable when the superasaturation starts to decay, but can act as precusors of clusters with higher Boron content. This is clearly shown in fig. 9, where B_3I and B_3I_2 concentrations (in arbitrary units) have been plotted as a function of temperature and time. This behaviour is the consequence of the values adopted for the BICs emission energies. Table I shows a comparison of the values used in this model with different literatura data: a quite good agreement for the most important BIC species has been found. The main discrepancy is related to the formation of B_3I from B_3 + I reaction: this is not very important because B_3 formation is not energetically favorable as shown for example in fig. 6 where no B_3 has been found.

Fig. 7 shows the results of the KMC simulations for the case of B 2e15 at/cm^2 at 20 keV annealed at 900°C a quite good agreement with data taken from [7] is found for three different times (30 sec, 30 min and 2 hour). Here the immobile peak reduces and starts to diffuse while intrinsic boron diffusivity

Table I: BICs emission energy

Reaction	This work	[9]	[10]	[11]	[12]
$BI_2 \rightarrow Bi+I$	2.4	2.0	1.33	2.0	1.4
$B_2I \rightarrow B+Bi$	2.156	2.23	1.1	1.5	0
$B_2I \rightarrow B_2+I$	3.656	3.03	3.05	2.9	0.6
$B_2I_2 \rightarrow Bi+Bi$	3.756	3.17	1.2	2.0	1.8
$B_2I_2 \rightarrow B_2I+I$	2.7	1.41	1.12	1.0	2.4
$B_2I_3 \rightarrow BI_2+Bi$	2.916	3.07	n.a.	3.0	0.4
$B_2I_3 \rightarrow B_2I_2+I$	1.56	1.9	n.a.	3.0	0
$B_3I \rightarrow B_2+Bi$	4.242	3.91	3.0	5.2	3.0
$B_3I \rightarrow B_3+I$	8.592	n.a.	3.98	7.0	3.05
$B_3I_2 \rightarrow B_2I+Bi$	3.418	3.25	1.27	1.6	4.6
$B_3I_2 \rightarrow B_3I+I$	2.832	2.37	1.32	-0.7	2.2
$B_3I_3 \rightarrow B_2I_2+Bi$	2.29	3.34	n.a.	3.1	4.2
$B_3I_3 \rightarrow B_3I_2+I$	1.572	1.5	n.a.	2.5	2.0

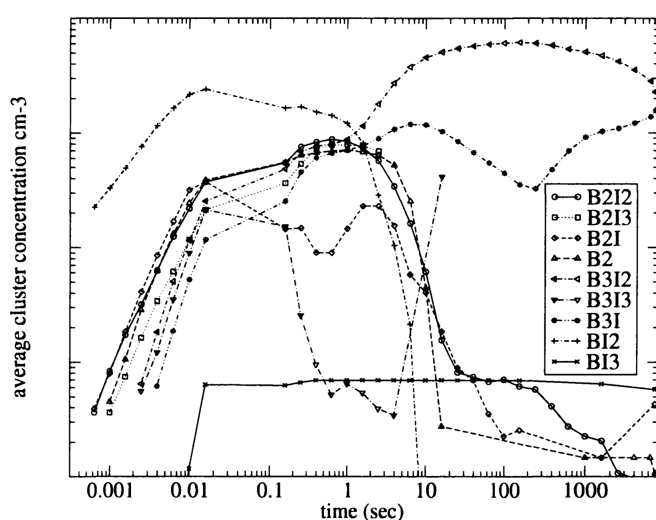

Figure 6: BiCs kinetics for the diffusion at 800°C corresponding to fig. 4 (B 2e15 at/cm^2 at 20keV), calculated as an average on the silicon top 0.8 μm.

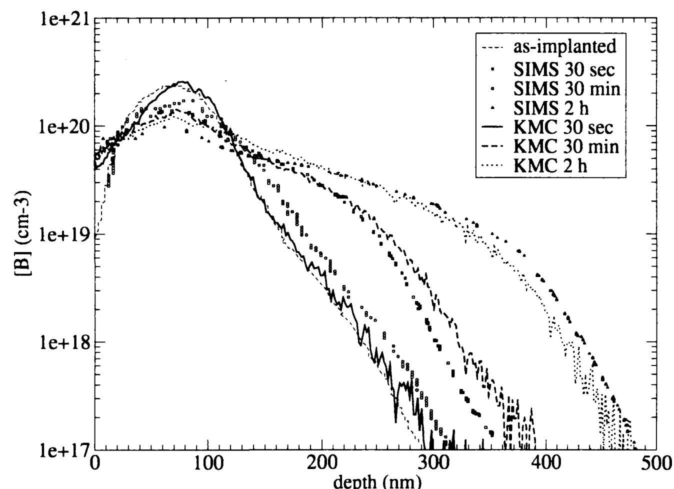

Figure 7: Comparison between simulations and experiment for Boron diffusion at 900°C (B 2e15 at/cm^2 at 20keV), ref. [7].

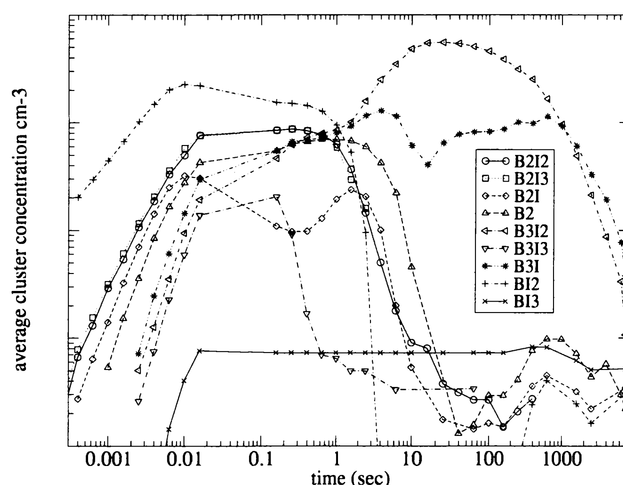

Figure 8: BiCs kinetics for the diffusion at 900°C corrisponding to fig. 7 (B 2e15 at/cm^2 at 20keV), calculated as an average on the silicon top 0.8 μm.

controls the long time evolution of Boron below the solubility limit. The increase of the dopant activation (from 78% to 99%) is mainly due the B_3I and B_3I_2 dissolution at long time, as shown in fig.8, where most of the BICs concentration reduce well below to the Boron concentration value for time $\geq 10^3$ sec.

Fig. 9 shows B_3I and B_3I_2 kinetics for temperatures between 700°C and 900°C ; three regions can be easily distinguished. A transient initial stage where BICs are growing is been followed by a plateaux where BICs are stable: the duration of the region depends on the temperature. The last zone is related to the temperature activated BICs dissolution process. Fig. 10 shows RTP annealing (10sec at 1000°C) from [7] corresponding to an implant of 5e14 at/cm^2 at 20 keV. The agreement with data is not so good as for the previous cases due to a too high B_3I and B_3I_2 concentration. It would be possible to obtain a better fit by changing cluster emission energy for such condition, but we preferred to use the same BICs emission energy for consistency reason.

The last two figures show the comparison of the atomistic simulations with spike processing: the case at 1000°C is from ref. [8] corresponding to a B 1e15 at/cm^2 implant at 500 eV, while the case at 1100°C is been based on our own experiment: B 5e14 at/cm^2 at 1keV, with ramp-up rate of 250 °C/sec and ramp-down rate of 60 °C/sec. To achieve a good agreement with the experimental data we reduced the critical (B_3I and B_3I_2) formation energies (thereby increasing their solubility) with respect to the values optimised for the furnace and RTA samples. Also in this conditions B_3I and B_3I_2 are (as in [8]) the most stable BICs, but their final concentration is substantially lower. We argue that because supersaturation vanishes already during rump-up, as shown in Fig. 1, higher order Boron clusters (not considered in this model) such as B_mI_n with m,n ≥ 4 could help in the control of the immobile part because of their high binding energy, and could allow to use the same formation energy of the B_3I and B_3I_2 clusters adopted in the other cases.

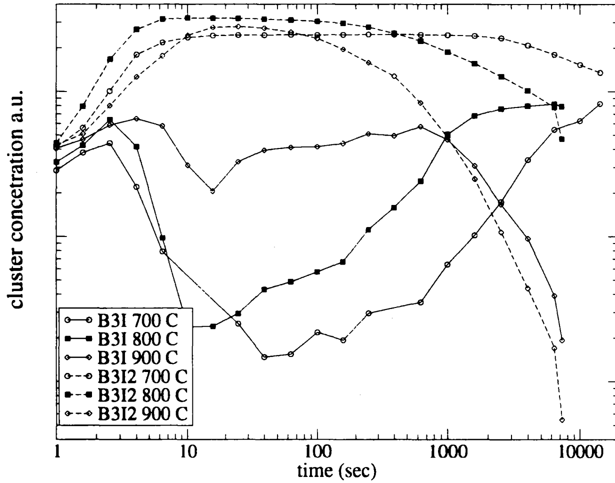

Figure 9: B_3I and B_3I_2 kinetics for different temperature as results of our simulation normalized for implanted dose.

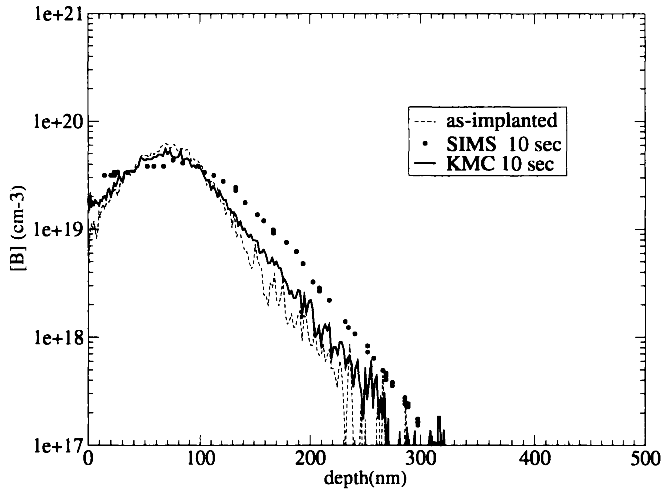

Figure 10: Boron diffusion at 1000°C (B 5e14 at/cm^2 at 20keV), ref. [7].

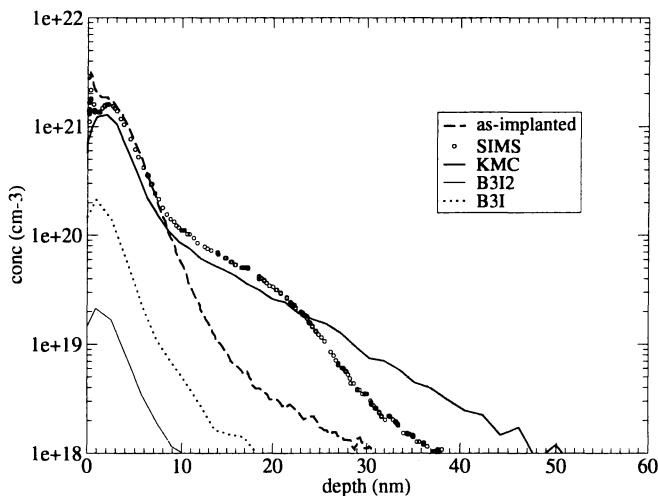

Figure 11: Boron spike diffusion at 1000°C for (B 1e15 at/cm^2 at 500 eV), ref. [8].

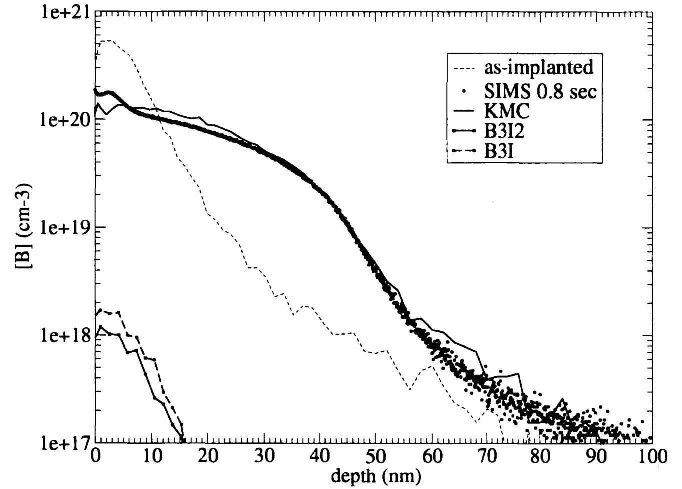

Figure 12: Boron spike diffusion at 1100°C (B 5e14 at/cm^2 at 1keV).

IV. Conclusion

Using a Kinetic Monte Carlo code a wide range of Boron diffusion experiments has been reproduced considering furnace, RTP and spike anneals. Our model and the unique setting of parameters is able to reproduce both boron enhanced diffusion and its transient activation in the case of standard annealing treatments. For the spike anneals a correction of the most important BICs was needed. Model and parameters have been compared with literature data.

Acknowledgment

The authors would like to thank Nikolas Zographos and Detlef Conrad of Synopsys Switzerland for their help in the beginning of the calibration procedure.

References

[1] S. Chakravarthi et al., *A simple continuum model for boron clustering based on atomistic calculations*, JAP 89 p.3650, 2001

[2] S.C. Jain et al., *Transient enhanced diffusion of boron in Si*, APR 91 p.8919, 2002

[3] *Synopys SProcess user guide*, 2008

[4] N. E. B. Cowern et al., PRL 82 p.4460, 1999

[5] M. L. Polignano et al., *The evolution of the ion implantation damage in device processing*, proc of DRIP XII, Berlin, 2007

[6] S.Solmi and M.Bersani, *Effects of donor concentration on transient enhanced diffusion of boron in silicon*, JAP 87 p.3696, 2000

[7] S.Solmi et al, *Diffusion of boron in silicon during post implantation anneal*, JAP 69 p.2135, 1991

[8] W.Lerch et al., *Experimental and theoretical results of dopant activation by a combination of spike and flash annealing*, proc of IWJT, 2007

[9] M.Cogoni et al., *Atomistic study of the dissolution of small boron interstitial cluster in c-Si*, APL 87 p.1912, 2005

[10] Thomas J. Lenosky et al., *Ab initio energetics of boron-interstitial clusters in crystalline Si*, APL 77 p.1834, 2000

[11] Xiang-Yang Liu et al., *Ab initio modeling of boron clustering in silicon*, APL 77 p.2018, 2000

[12] L. Pelaz et al,. *B cluster formation and dissolution in Si: A scenario based on atomistic modeling*, APL 74 p.3657, 1999